Global and Specific Translational Regulation in the Genomic Response of *Saccharomyces cerevisiae* to a Rapid Transfer from a Fermentable to a Nonfermentable Carbon Source

KENNETH M. KUHN,[1] JOSEPH L. DeRISI,[2]† PATRICK O. BROWN,[2]* AND PETER SARNOW[1]*

Department of Microbiology and Immunology[1] and Department of Biochemistry and Howard Hughes Medical Institute,[2] Stanford University School of Medicine, Stanford, California 94305

The global gene expression program that accompanies the adaptation of *Saccharomyces cerevisiae* to an abrupt transfer from a fermentable to a nonfermentable carbon source was characterized by using a cDNA microarray to monitor the relative abundances and polysomal distributions of mRNAs. Features of the program included a transient reduction in global translational activity and a severe decrease in polysome size of transcripts encoding ribosomal proteins. While the overall translation initiation of newly synthesized and preexisting mRNAs was generally repressed after the carbon source shift, the mRNA encoded by *YPL250C* was an exception in that it selectively mobilized into polysomes, although its relative abundance remained unchanged. In addition, splicing of *HAC1* transcripts, which has previously been reported to occur during accumulation of unfolded proteins in the endoplasmic reticulum, was observed after the carbon shift. This finding suggests that the nonconventional splicing complex, composed of the kinase-endonuclease Ire1p and the tRNA ligase Rlg1p, was activated. While spliced *HAC1* transcripts mobilized into polysomes, the vast majority of unspliced *HAC1* RNA accumulated in nonpolysomal fractions before and after the carbon source shift, indicating that translation of unspliced *HAC1* RNA is blocked at the translation initiation step, in addition to the previously reported elongation step. These findings reveal that *S. cerevisiae* reacts to the carbon source shift with a remarkable variety of responses, including translational regulation of specific mRNAs and activation of specific enzymes involved in a nonconventional splicing mechanism.

Saccharomyces cerevisiae ferments glucose, producing ethanol and CO_2, even under aerobic conditions (24, 28). The mechanisms by which this yeast senses the presence of glucose and regulates the expression of genes required for glucose uptake and metabolism and for repression of respiratory pathways are complex and are under intense scrutiny (23).

After it consumes all available glucose, *S. cerevisiae* uses ethanol, the product of fermentation, as a carbon source for aerobic growth. This "diauxic shift" is characterized by a transient cell cycle arrest and a metabolic adaptation to respiratory growth (40, 41). The post-diauxic-shift growth phase is characterized by one to three doublings over a period of 1 week, after which cells enter stationary phase, during which the yeast genome remains unreplicated (40, 41). While overall rates of transcription and translation are diminished in stationary-phase cells (17, 39), the abundances of transcripts of some stress-responsive genes are increased (5, 39). Interestingly, it has been reported that certain mRNAs are translated with equivalent efficiencies during exponential growth and stationary phase (14, 17), implying that translational control may also play a role in response to starvation or cell stress. More recently, cDNA microarrays were used to examine changes in

gene expression that occur during the diauxic shift (13). This analysis has identified many mRNAs whose relative abundances were upregulated, such as those involved in respiratory metabolism, or downregulated, such as those involved in protein biosynthesis (13).

Although entry into stationary phase as a result of gradual glucose exhaustion has been widely investigated, much less is known about the biochemical and physiological consequences of abrupt withdrawal of *S. cerevisiae* from a fermentable carbon source. When faced with such a situation, the organism must react with quick adaptive responses to ensure its survival. In addition to transcriptional changes in gene expression patterns, translational regulation would allow an immediate response to sudden environmental stresses by rapidly increasing or decreasing the production of specific proteins. For example, the mRNA encoding the transcription factor Gcn4p, which upregulates the transcription of genes involved in amino acid biosynthesis, becomes selectively translated following amino acid deprivation (reviewed in reference 19).

Translational control during glucose starvation has recently received attention because the signaling pathways that lead to global reduction in protein synthesis have begun to be deciphered (1). We therefore investigated the changes in overall abundance, as well as the translational activity of individual mRNAs, as yeast cells adapt to the shift from glucose to glycerol as the sole carbon source.

MATERIALS AND METHODS

Yeast strains and media. Yeast strains used in this study include MBS (*MATα ade2-1 his3-11,15 leu2-3,112 trp1-1 ura3-1 can1*) (21); YCS243a (ΔIRE1) (*MATα*

---

* Corresponding author. Mailing address: Department of Microbiology and Immunology, Stanford University School of Medicine, Stanford, CA 94305. Phone: (650) 498-7076. Fax: (650) 498-7147. E-mail for Peter Sarnow: psarnow@leland.stanford.edu. E-mail for Patrick O. Brown: pbrown@cmgm.stanford.edu.

† Present address: Department of Biochemistry and Biophysics, University of California at San Francisco, San Francisco, California 94116.
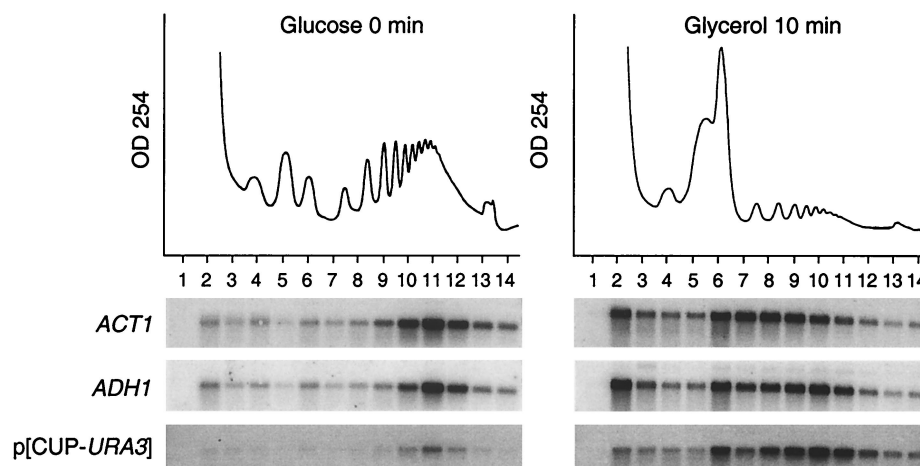
FIG. 1. Polysomal association of mRNAs in yeast cells grown exclusively in glucose medium or after a 10-min shift to glycerol medium. Absorbance profiles at 254 nm of the collected sucrose gradients are shown above the panels. Fourteen equal-volume fractions were collected from each gradient (fraction 1 is the top of the gradient), and purified RNAs were analyzed by Northern blotting. The levels of *ACT1*, *ADH1*, and *URA3* mRNAs were visualized by a phosphorimage of the Northern blot. The *CUP1* promoter was induced by addition of 10 mM CuSO$_4$ to the glycerol medium (but not to the glucose medium).

ade2-1 his3-11 leu2-3,112::LEU2 UPRE-LACZ trp1-1 ura3-1 can1-100 ire1::URA3) (obtained from P. Walter, University of California, San Francisco); YCS243a (ΔIRE1) transformed with pCS110, which contains the *IRE* gene and a *TRP* marker gene (also from P. Walter); CML240 (*MATa ade2-1 his3-11 leu2-3,112::LEU2 CMVp(tetR′-SSN6) trp1-Δ2 ura3-1 can1-100*) (obtained from E. Herrero, Universitat de Lleida), and CML240 transformed with pCM184 (also from E. Herrero), which contains a *URA3V5H6* reporter (described below) and a *TRP* marker. Cells were grown at 30°C in a synthetic minimal medium composed of 1.7 g of yeast nitrogen base (Difco)/liter, lacking amino acids, supplemented with 5 g of ammonium sulfate/liter. Selected components (adenine at 40 μg/ml, histidine at 20 μg/ml, leucine at 60 μg/ml, tryptophan at 40 μg/ml, uracil at 20 μg/ml [2], and 2% [wt/vol] glucose) were added when needed. Doxycycline was added to a final concentration of 2 μg/ml (3). Yeast cells for all experiments were harvested at mid-log phase (optical density at 595 nm OD$_{595}$ 0.5). For carbon source shifts, cells were first sedimented at 5,000 × g and 20°C for 5 min (the lower temperature prevented overheating during centrifugation). The cell pellets were immediately resuspended in the synthetic minimal medium, prewarmed to 30°C, in which glucose had been replaced with 2% (wt/vol) glycerol.

PCR and cloning. The *HAC1* intron was amplified by PCR from yeast genomic DNA, using forward (5′-CGTGATTACGATGACCAGGAAAC-3′) and reverse (5′-CAGTACAAGCCGTCCATTTC-3′) primers, under the following cycling conditions: 65°C for 1 min, 75°C for 1 min, and 95°C for 1 min for 25 cycles. These cycling parameters were used for all PCRs.

Plasmid p(CUP-URA) was constructed by first amplifying the complete *URA3* open reading frame (ORF) from yeast genomic DNA with forward (5′-CTAG CTCGAGAAAATGTCGAAAGCTACATATAAGG-3′) and reverse (5′-CTA GGCATGCTTAGTTTTGCTGGCCGCATCTTC-3′) primers. The PCR product was purified, digested with *Xho*I and *Sph*I, and ligated into plasmid pSAL1 (32) previously digested with *Xho*I and *Sph*I (restriction sites in primers are underlined).

Plasmid p(5′cyc-ura3-cyc3′) was constructed by first amplifying the complete *URA3* ORF with forward (5′-CTAGGGATCCAAAATGTCGAAAGCTACAT ATAAGG-3′) and reverse (5′-CTAGGGTGACCTCGAAGCTCGCCCTTGTT TTGCTGGCCGCATCTTC-3′) primers. The PCR product was purified and digested with *Bam*HI and *Bst*EII. The *URA3* ORF was extended 99 nucleotides by an in-frame fusion with a dual V5 six-His tag, isolated by digesting pYES2/GS (GeneStorm; Invitrogen) with *Bst*EII and *Pst*I (the *Xba*I site of pYES/GS had been changed to a *Pst*I site by site-directed mutagenesis). The above-described DNA fragments were cloned, by three-part ligation, into pCM184 (3) previously digested with *Bam*HI and *Pst*I.

RNA isolation and Northern analysis. For total-RNA isolation, 10-ml cultures were pelleted at 5,000 × g and the cell pellets were frozen on dry ice. Total RNA was extracted by the hot acid phenol method (2). Eight micrograms of total RNA was fractionated on a 1.2% agarose-formaldehyde gel (2), then transferred to a Zeta-probe membrane (Bio-Rad) for 1 h by the use of a pressure blotter (Stratalinker; Stratagene). RNA was cross-linked to the membrane by UV (254

nm) irradiation at an energy setting of 120 mJ (Stratagene). The integrity of the RNA and the efficiency of transfer were evaluated by staining the membrane with 0.3% methylene blue (2).

For Northern analysis, full-length yeast ORFs (Research Genetics) or *Hac*I intron PCR products were radiolabeled by using a RadPrime labeling kit (Gibco BRL) and purified by PCR purification column chromatography (Qiagen). Standard hybridization was performed overnight at 65°C in a solution containing 500 mM Na$_2$HPO$_4$ (pH 7.2), 1 mM EDTA, and 7% (wt/vol) SDS. The blots were washed twice in 40 mM Na$_2$HPO$_4$ (pH 7.2) containing 1 mM EDTA, and 5% (wt/vol) sodium dodecyl sulfate (SDS) (Bio-Rad) for 15 min each time and twice in 40 mM Na$_2$HPO$_4$ (pH 7.2) containing 1 mM EDTA and 1% (wt/vol) SDS (Bio-Rad) for 15 min each time. All washes were performed at 65°C. For oligodeoxynucleotide hybridization, 25 pmol of the *Hac*I "splice oligo" (5′-CTG CGCTTCTGGATTACG-3′) was labeled with T4 kinase [γ-^{32}P]ATP at 6,000 Ci/mmol and purified by using a Qiagen nucleotide removal kit. Hybridization was performed in a solution containing 5× SSC (1× SSC is 0.15 NaCl plus 0.015 M sodium citrate), 20 mM Na$_2$HPO$_4$ (pH 7.2), 1× Denhardt's solution, 7% (wt/vol) SDS, and 100 mg of denatured salmon sperm DNA/ml overnight at 50°C. The blots were washed twice in a solution consisting of 3× SSC, 25 mM Na$_2$HPO$_4$ (pH 7.2), 10× Denhardt's solution, and 5% SDS at 50°C for 30 min each time and then once in 1× SSC–1% (wt/vol) SDS at 50°C for 30 min. Quantitation was performed with a Storm PhosphorImager and ImageQuant software (Molecular Dynamics).

Polysome analysis. Material from 75-ml cultures (OD$_{595}$0.6) was used for each sucrose gradient. At the time of harvest, cycloheximide (Sigma) was added to a final concentration of 0.1 mg/ml, and the cultures were chilled on ice for 5 min. Cells were pelleted by centrifugation at 5,000 × g and 4°C for 5 min. The cell pellet was then resuspended in 3 ml of polysome extraction buffer (20 mM Tris-HCl [pH 8.0], 140 mM KCl, 5 mM MgCl$_2$, 0.5 mM dithiothreitol [DTT], 1% [vol/vol] Triton X-100, 0.1 mg of cycloheximide/ml, and 1 mg of heparin/ml) and sedimented. This washing step was repeated, and the final cell pellet was resuspended in 750 μl of ice-cold polysome extraction buffer and transferred to a chilled 15-ml Corex glass tube containing a 500-μl volume of acid-washed 0.45- to 0.55-mm-diameter glass beads (Sigma). All subsequent steps were performed on ice with prechilled extraction buffer. The reaction mixture was vortexed at full speed for 20 and then incubated on ice for 100 s. This process was repeated three times. After cell lysis, glass beads and excess cell debris were removed by sedimentation in a microcentrifuge at 3,500 × g and 4°C for 5 min. The supernatant (approximately 0.5 ml) was transferred to a 1.7-ml microcentrifuge tube containing 0.5 ml of extraction buffer and vortexed vigorously. The sample was clarified by sedimentation in a microcentrifuge at 8,000 × g and 4°C for 5 min. Approximately 0.8 ml of sample was layered onto an 11-ml 10 to 50% (wt/vol) sucrose gradient that contained extraction buffer lacking Triton X-100. The sample was sedimented at 35,000 rpm and 4°C in an SW41 rotor for 160 min. Gradient fractions were collected as described previously (22) with minor modifications. Briefly, 14 0.9-ml fractions were collected directly into 2-ml volumes of 8 M
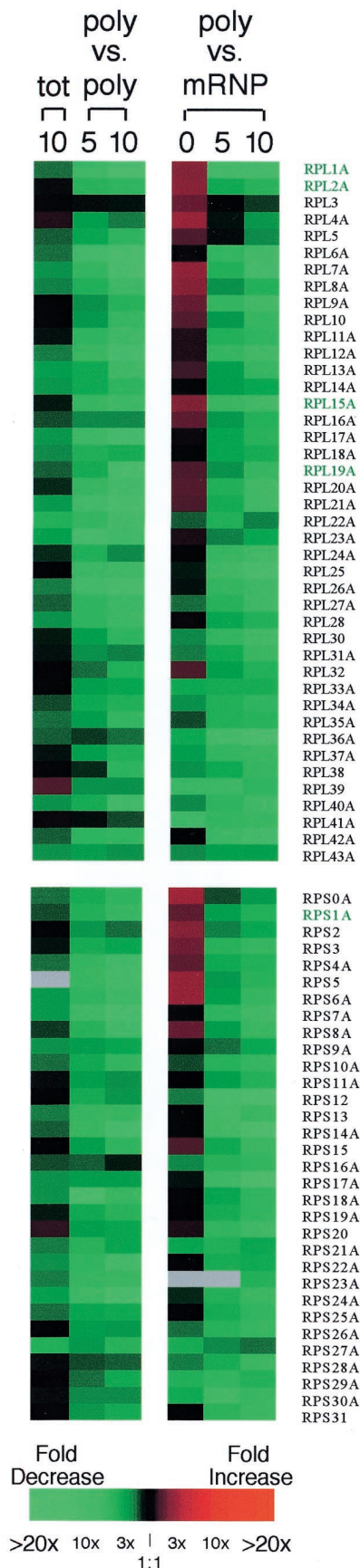
guanidine-HCl. After the fractions were vortexed, 3 ml of 100% ethanol (EtOH) was added to each tube, and the samples were vortexed vigorously and stored overnight at −20°C to precipitate the RNA. The pellets were collected by sedimentation, washed in 75% EtOH, resuspended in 0.4 ml of Tris-EDTA (TE; pH 8.0), and transferred to 1.7-ml Eppendorf tubes. The RNA was again precipitated by addition of 50 μl of 3 M sodium acetate (pH 5.2) and 1 ml of 100% EtOH. Each RNA pellet was washed in 75% EtOH and resuspended in TE (pH 8.0) to a final volume of 25 μl. Equal volumes of all samples were analyzed by Northern analysis.

cDNA microarray analysis. Template RNA was converted to cDNA by reverse transcriptase, and Cy3-dUTP or Cy5-dUTP was incorporated into second-strand cDNA with the Klenow fragment of DNA polymerase as described previously (15). Briefly, purified template RNA (see below) in deionized water (dH₂O) was denatured at 70°C for 10 min and then incubated on ice for 1 min. First-strand cDNA was synthesized in reverse transcription buffer, containing 6 μg oligo (dT)$_{18}$ (New England Biolabs), 50 mM Tris-HCl (pH 8.3), 75 mM KCl, 3 mM MgCl$_2$, 10 mM DTT, 0.5 mM each deoxynucleoside triphosphate and 400 U of SuperScript II RNase H-free reverse transcriptase (Gibco BRL) in a final volume of 30 μl. The reaction was performed at 42°C for 2 h. Template RNA was degraded by adding 15 μl of 0.1 M NaOH and incubating at 70°C for 10 min. The mix was neutralized by adding 15 μl of 0.1 M HCl, diluted with 500 μl of TE, and concentrated to a volume of 20 to 30 μl in a Microcon 30 microconcentrator (Amicon). The dilution and concentration steps were repeated once. The sample was then denatured at 100°C for 1 min and allowed to cool at room temperature for 5 min. A Cy3- or Cy5-deoxynucleoside triphosphate fluor was incorporated in Klenow buffer (containing 12 μg of random nanomer [Research Genetics]; 10 mM Tris-HCl [pH 7.4]; 5 mM MgCl$_2$; 7.5 mM DTT; 0.025 mM each dATP, dCTP, and dGTP; 0.009 mM dTTP; 0.03mM Cy3- or Cy5-dUTP; and 10 U of exonuclease-free Klenow enzyme [U. S. Biochemicals] [final volume, 50 μl]). The reaction was performed at 37°C for 2 h, and the samples were purified as described above. The Cy3- or Cy5-labeled cDNAs were then combined, diluted with 500 μl of TE, and concentrated to a final volume of 10 to 20 μl. Microarray hybridization was performed overnight at 65°C in a buffer containing 1.6 μg of poly(A) (Sigma)/ml 3.5× SSC, and 0.3% (wt/vol) SDS. The microarrays were washed at room temperature for 2 min each in 2× SSC, 0.1% SDS (wash 1), 1× SSC (wash 2), and 0.2× SSC (wash 3); spun dry in a centrifuge; and scanned with a GenePix 4000A microarray scanner (Axon Instruments). Cluster analysis was performed with ScanAlyze software (M. Eisen [16]; available at http://genome-www4.stanford.edu/MicroArray/SMD/index.html).

For comparison of total RNA abundances, 20 μg of total RNA was used as a template in the first-strand cDNA reaction. For comparison of polysomal RNA abundances, additional purification steps were necessary prior to first-strand cDNA synthesis. First, to obtain equal amounts of polysomal RNA (roughly 20 μg), polysomal fractions 10 through 14 eluted from three glucose and six glycerol gradients were pooled for each time point. This design gave a slight enrichment of mRNAs isolated from glycerol polysomes. The pooled samples were then diluted to 0.65 ml with dH₂O and extracted with 0.65 ml of Tris-buffered phenol-chloroform. The resultant aqueous phase (approximately 0.5 ml) was diluted to 1 ml with H₂O and LiCl (added to a final concentration of 1.5 M). RNA was allowed to precipitate overnight at −20°C. The samples were thawed at 4°C and

FIG. 2. Expression of ribosomal-protein-encoding (RP) mRNAs in yeast cells after the carbon source shift. Each colored square represents the ratio of total mRNA (tot) or high-molecular-weight polysomal mRNA (poly vs. poly; fractions 10 to 14) isolated following incubation in glycerol medium for 5 or 10 min, relative to the amount of the mRNA isolated from cells grown in the presence of glucose. In addition, mRNA abundance in fractions 2 through 6, designated as mRNA protein complexes (mRNP), was compared to the abundance of mRNA present in polysomes (poly vs. mRNP). Black squares denote no significant difference in the amount of RNA isolated from glucose-grown or glycerol-shifted cells; red squares and green squares denote RNAs that are more or less abundant, respectively. The intensity of the color is proportional to the log$_2$ of the fold increase or decrease, with maximal intensity corresponding to an eightfold increase or decrease. For duplicated RP mRNA genes (designated A and B), only data for the A gene are presented. The cDNA for *RPL29* (YFR032CA) was not included in this batch of microarrays. A gray box indicates an unreadable spot on the microarray. The color intensity scale was adapted from reference 9. Selected RP mRNAs (highlighted in green) were chosen for further analysis.
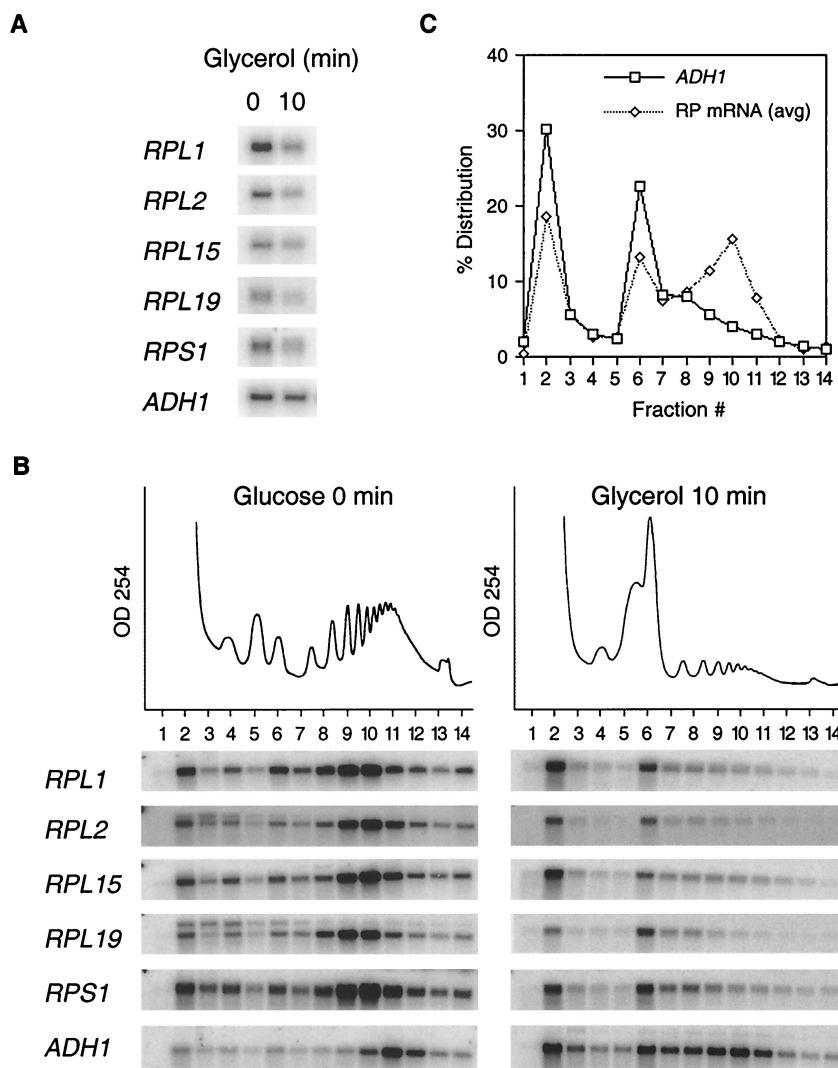
FIG. 3. Relative abundances and translational activities of selected RP mRNAs as a function of time following transfer to glycerol medium. (A) Total levels of RP mRNAs (*RPL1, RPL2, RPL15, RPL19*, and *RPS1*), as well as a control *ADH1* mRNA, after Northern blot hybridization are displayed. (B) Polysome association of RP mRNAs. For details, see the legend to Fig. 1. The Northern blot displaying *ADH1* mRNA was taken from Fig. 1. Phosphorimages of the Northern blots are shown. (C) Quantitation of polysomal distribution of averaged RP and *ADH1* mRNAs after the shift to glycerol medium (panel B). The data points represent the percent intensity of each fraction relative to the total combined intensity of all fractions for each gradient. The five RP data sets from panel B were combined and averaged to give a general polysomal distribution pattern for the selected RP mRNAs.

pelleted at high speed in a 4°C microcentrifuge for 15 min. Each purified RNA pellet was washed with 75% ethanol, air dried, resuspended in 0.15 ml of dH$_2$O by repeated freezing and thawing, and then precipitated by addition of 20 µl of sodium acetate (pH 5.2) and 0.45 ml of 100% EtOH. The final RNA pellets were each resuspended in 25 µl of 1 mM Tris (pH 8.0). For comparison of polysomal and nonpolysomal RNA abundances, RNA was isolated from fractions 2 through 6 and compared directly to RNA isolated from fractions 10 through 14 of the same gradient. For each time point, material from three gradients was pooled and processed identically to minimize enrichment (6). The microarray data are available on the World Wide Web at http://genome-www4.stanford.edu/MicroArray/SMD/publications.html.

RESULTS

Withdrawal of glucose leads to a global translational repression. To monitor the effect of the carbon source shift on protein synthesis, the overall rate of [^{35}S]methionine incorpora-

tion was examined at various time points after the switch from glucose to glycerol medium. Protein synthesis was transiently reduced by approximately 80% at 5 min after the shift to glycerol medium and increased again by two- to threefold at 15 min after the shift, but it did not return to the level observed in exponentially growing cells (data not shown). Thus, an abrupt shift from glucose to glycerol resulted in a rapid, transient reduction of protein synthesis, in agreement with data published by Ashe et al. (1).

To test whether decreased protein synthesis was a consequence of a decreased translation rate, we examined the global distribution of ribosomes and ribosomal subunits, as well as the polysomal distribution of several individual mRNAs, such as *ACT1* and *ADH1* (Fig. 1). Following the carbon source shift, there was a global redistribution of ribosomes from polysomes
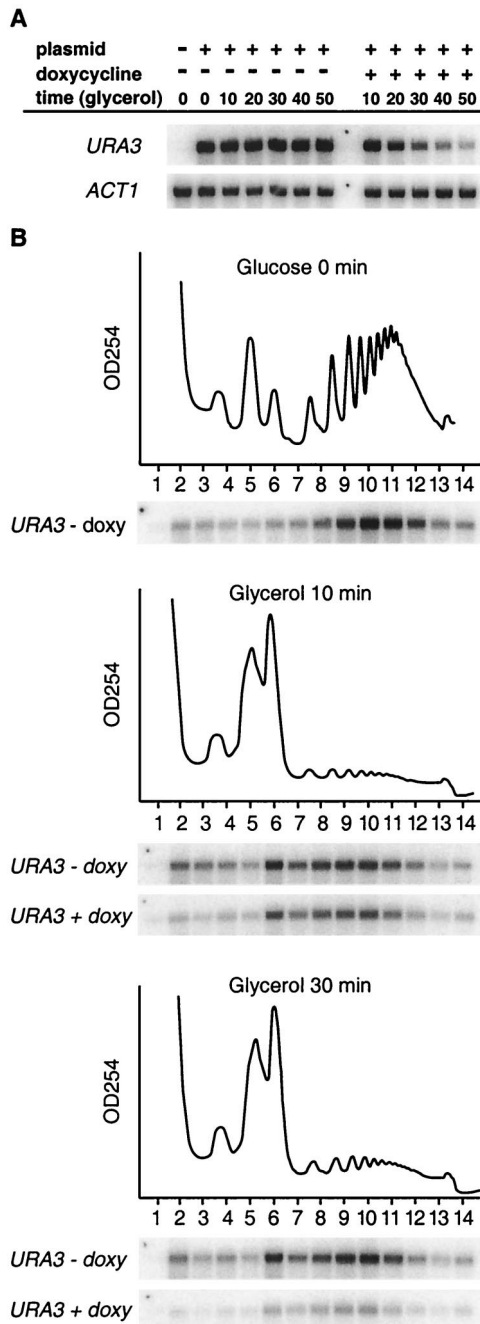
FIG. 4. Decreasing the abundance of an mRNA does not decrease its translational efficiency. (A) Total levels of *URA3* and *ACT1* mRNAs at various time points after addition of the tetracycline analogue doxycycline (2 μg/ml) to yeast cells grown in glycerol medium are shown. (B) Polysomal distribution of *URA3* mRNA in yeast cells grown in glycerol medium in the presence (+) or absence (−) of doxycycline (doxy). The plasmid-derived *URA* mRNA was distinguished from the endogenous *URA3* mRNA by using a probe complementary to a V5 six-His extension of the plasmid coding sequence (see Materials and Methods).

toward 80S monosomes and dissociated 40S and 60S subunits (Fig. 1). The majority of 80S monosomes that accumulated after the shift could be dissociated in the presence of 0.8 M KCl (K. Kuhn, unpublished data), indicating that they were not

engaged in the translation of mRNAs. In addition to the global loss of polysomes, the average polysome size (number of ribosomes per mRNA) was reduced as well, as exemplified by the slower sedimentation rate of *ACT1* and *ADH1* mRNAs. These findings indicate that the carbon source shift resulted in a decrease in the rate of translation initiation.
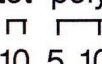
To test the possibilities that translation initiation was completely inhibited and that the remaining polysomal association of mRNAs was due to residual elongating ribosomes, we examined whether a newly synthesized mRNA could be translated at the time of the carbon source shift. *URA3* mRNA, expressed at low levels from an uninduced *CUP1* promoter, sedimented with high-molecular-weight polysomes (Fig. 1, fraction 11) prior to glucose withdrawal. New *URA3* mRNA, synthesized following induction of the *CUP1* promoter at the time of the carbon source shift, was predominantly polysome associated, although it was associated with fewer ribosomes (Fig. 1, fractions 9 to 11) than in the control, glucose-grown cells. The simplest interpretation of these findings is that translation initiation was markedly reduced after the shift from a fermentable to a nonfermentable carbon source but did not completely cease.

Relative abundance and polysomal association of ribosomal mRNAs are coordinately repressed after the carbon source shift. Other reasons for the reduced overall amount of translation after the carbon source shift might include a rapid loss of certain abundant mRNA species in the cell. To examine this possibility, the relative abundance and polysomal association of mRNAs were examined after the shift from glucose to glycerol medium, using a cDNA microarray (12, 13, 15). Of the approximately 6,275 mRNAs examined, 120 mRNA species consistently showed a greater than twofold reduction in polysomal association in at least four cDNA microarray experiments (Fig. 2); 89 of those mRNAs encode ribosomal proteins.

It is known that the abundance of ribosomal protein (RP) mRNAs rapidly decreases when yeast cells encounter stress situations such as heat shock (18, 19, 27), diauxic shift (13, 26), or inhibition of the secretory pathway (30, 34). It has been argued that the rapid changes in intracellular concentrations of RP mRNAs are due to transcriptional repression, along with constitutively fast mRNA turnover (19, 27, 29, 35). Recently, Li et al. (29) pointed out that the 137 yeast RP genes contributed 30% of the total mRNA in the cell. Considering that the turnover rate of an average RP mRNA is 5 to 7 min (29), inhibition of transcription of RP genes might diminish the intracellular concentration of RP mRNAs within several minutes. As a result, the amount of polysomes would decrease by as much as 30% and excess 80S ribosomes and ribosomal subunits would accumulate in the cell.

The cDNA microarray analysis revealed that the total abundances of most RP mRNAs decreased rapidly, by 10 min after the carbon source shift (Fig. 2). When the partial concentrations of RP mRNAs, as a fraction of all polysomal mRNAs, of samples taken before and after the carbon source shift were directly compared, (Fig. 2), almost all RP mRNAs showed a striking decrease in their relative abundances in polysomes after the carbon source shift. To determine whether the decrease in polysome-associated RP mRNA simply reflected the decrease in total RP mRNA abundance or reflected a redistribution to nonpolysomal fractions, the relative abundance of

A

poly
vs.
tot　poly

10　5　10

Metabolic

ORF	Gene	Function	Cellular Role
YBR145W	ADH5	Alcohol Dehydrogenase	Glycolysis
YCL040W	GLK1	Glucokinase	Glycolysis
YFR053C	HXK1	Hexokinase	Glycolysis
YDL021W	GPM2	Phosphoglycerate Mutase	Glycolysis
YMR105C	PGM2	Phosphoglucomutase	Glycolysis
YOR347C	PYK2	Pyruvate Kinase	Glycolysis
YFR015C	GSY1	Glycogen Synthase	Glycogen Metabolism
YLR258W	GSY2	Glycogen Synthase	Glycogen Metabolism
YKR058W	GLG1	Glycogen Synthesis Initiator	Glycogen Metabolism
YOR178C	GAC1	Glc7p Regulatory Subunit	Glycogen Metabolism
YPR160W	GPH1	Glycogen Phosphorylase	Glycogen Metabolism
YDL022W	GPD1	Glycerol-3-Phosphate dehydrogenase	Glycerol Metabolism
YBR126C	TPS1	Trehalose-6-Phosphate Synthase	Trehalose Metabolism
YDR074W	TPS2	Trehalose-6-Phosphate Phosphatase	Trehalose Metabolism
YML100W	TSL1	Trehalose-6-Phosphate Phosphatase/Synthase	Trehalose Metabolism
YGR194C	XKS1	Xylulokinase	Xylulose Utilization
YMR170C	ALD2	Aldehyde Dehydrogenase	Ethanol Utilization
YMR169C	ALD3	Aldehyde Dehydrogenase	Ethanol Utilization
YOR347W	ALD4	Aldehyde Dehydrogenase (Mitochondrial)	Ethanol Utilization
YHL032C	GUT1	Glycerol Kinase	Glycerol Utilization
YIL155C	GUT2	Glycerol-3-Phosphate Dehydrogenase	Glycerol Metabolism
YNR001C	CIT1	Citrate Synthase	TCA Cycle
YOL126C	MDH2	Malate Dehydrogenase	TCA Cycle
YDR178W	SDH4	Succinate Dehydrogenase Anchor Subunit	TCA Cycle, Oxidative Phosphorylation
YML120C	NDI1	NADH-Ubiquinone-6 Oxidoreductase	Oxidative Phosphorylation
YER065C	ICL1	Isocitrate Lyase	Glyoxylate Cycle
YML054C	CYB2	Cytochrome-B2	Lactate Utilization
YKL150W	MCR1	Cytochrome-B5 Reductase	Electron Carrier
YDR513W	TTR1	Glutaredoxin	Electron Carrier
YGR008C	STF2	ATPase-Stabilizing Factor	ATP Synthesis
YBL015W	ACH1	Acetyl-CoA Hydrolase	Acetyl-CoA Metabolism
YBR149W	ARA1	Arabinose Dehydrogenase	Arabinose Metabolism
YOR317W	FAA1	Long Chain Fatty Acyl-CoA Synthetase	Fatty Acid Metabolism
YGR019W	UGA1	4-Aminobutyrate Aminotransferase	GABA Metabolism
YKL035W	UGP1	UDP-Glucose Pyrophosphorylase	Pyrimidine Metabolism

Transport

ORF	Gene	Function	Cellular Role
YHR094C	HXT1	Hexose Permease	Transport
YMR011W	HXT2	Hexose Permease	Transport
YDR345C	HXT3	Hexose Permease	Transport
YHR096C	HXT5	Hexose Permease	Transport
YDR343C	HXT6	Hexose Permease	Transport
YDR342C	HXT7	Hexose Permease	Transport
YKL217W	Jen1	Lactate Transporter	Transport
YGR289C	MAL11	Alpha-Glucoside Permease	Transport
YBR298C	MAL31	Maltose Permease	Transport
YDL194W	SNF3	Glucose Permease	Transport

Cell Stress

ORF	Gene	Function	Cellular Role
YNL160W	YGP1	Unknown, Response to Nutrient Limitation	Diauxic Shift
YOR028C	CIN5	Basic Leucine Zipper Transcription Factor	Salt Tolerance
YJL165C	HAL5	Protein Kinase (putative)	Salt Tolerance
YGR023W	MTL1	Unknown, Acts with Mid2p	Signaling (putative)

Heat Shock

ORF	Gene	Function	Cellular Role
YMR173W	DDR48	Unknown	Induced By DNA Damage, Heat Shock
YFL014W	HSP12	Heat Shock Protein	Glucose and Lipid Utilization
YCR021C	HSP30	Heat Shock Protein (Plasma Membrane)	Diauxic Shift
YDR171W	HSP42	Heat Shock Protein	Cytoskeleton Assembly
YDR258C	HSP78	Heat Shock Protein (Mitochondrial)	Protein Folding
YLL026W	HSP104	heat Shock Protein	Heat Shock response/Thermotolerance
YBR054W	YRO2	Heat Shock Protein (putative)	Unknown

Signaling

ORF	Gene	Function	Cellular Role
YFR014C	CMK1	Calmodulin-Dependent Protein Kinase	Signaling
YOL016C	CMK2	Calmodulin-Dependent Protein Kinase	Signaling
YGR070W	ROM1	GTP/GDP Exchange Protein for Rho1p	Signaling
YOR134W	BAG7	GTPase-Activating Protein	Signaling
YJL141C	YAK1	Serine-Threonine Protein Kinase	Signaling
YJL164C	TPK1	cAMP-Dependent Protein Kinase	Signaling
YPL203W	TPK2	cAMP-Dependent Protein Kinase	Signaling, Nutrient Control of Cell Growth
YNL098C	RAS2	GTP-Binding Protein, RAS Homolog	Signaling, RAS Pathway

Transcription

ORF	Gene	Function	Cellular Role
YKL109W	HAP4	Component of Heterotrimeric CCAAT-Binding Complex	Diauxic Shift
YKL043W	PHD1	Transcription Factor	Pseudohyphal Growth
YBR083W	TEC1	Transcription Factor	Pseudohyphal Growth
YGR249W	MGA1	Transcription Factor (putative)	Pseudohyphal Growth
YIL101C	XBP1	Transcriptional Repressor	Stress Response
YDR277C	MTH1	Transcriptional Repressor	Hexose Transport
YGL035C	MIG1	Transcriptional Repressor	Glucose Repression

B

Protein Degradation

	YBR286W	APE3	Vacuolar Aminopeptidase Y	Protein Degradation
	YKL103C	LAP4	Vacuolar Aminopeptidase YSC1	Protein Degradation
	YPL154C	PEP4	Vacuolar Aspartyl Protease	Protein Degradation
	YPL003W	ULA1	Rub1p Activating Protein	Protein Degradation, Rub1p-Mediated
	YEL012W	UBC8	E2 Ubiquitin-Conjugating Enzyme	Protein Degradation, Ubiquitin-Mediated
	YKR098C	UBP11	Ubiqitin-Specific Protease	Protein Degradation, Ubiquitin-Mediated

Miscellaneous

	YHR071W	PCL5	Cyclin (Pho85p)	Cell Cycle
	YLR178C	TFS1	Supresses CDC25 Mutations	Cell Cycle
	YEL011W	GLC3	Glycogen Branching Enzyme	Cell Wall Biogenesis
	YKL193C	SDS22	Glc7p Regulatory Subunit	Glucose Repression
	YDR085C	AFR1	Cytoskeletal Protein	Mating
	YMR081C	ISF1	Interacts with Nam7p	RNA Splicing (Mitochondrial)
	YNL036W	NCE103	Unknown	Secretion, Non-Classical
	YBR105C	VID24	Peripheral Vesicle Membrane Protein	Vacuolar Protein Targetting

Candidates for Translational Control

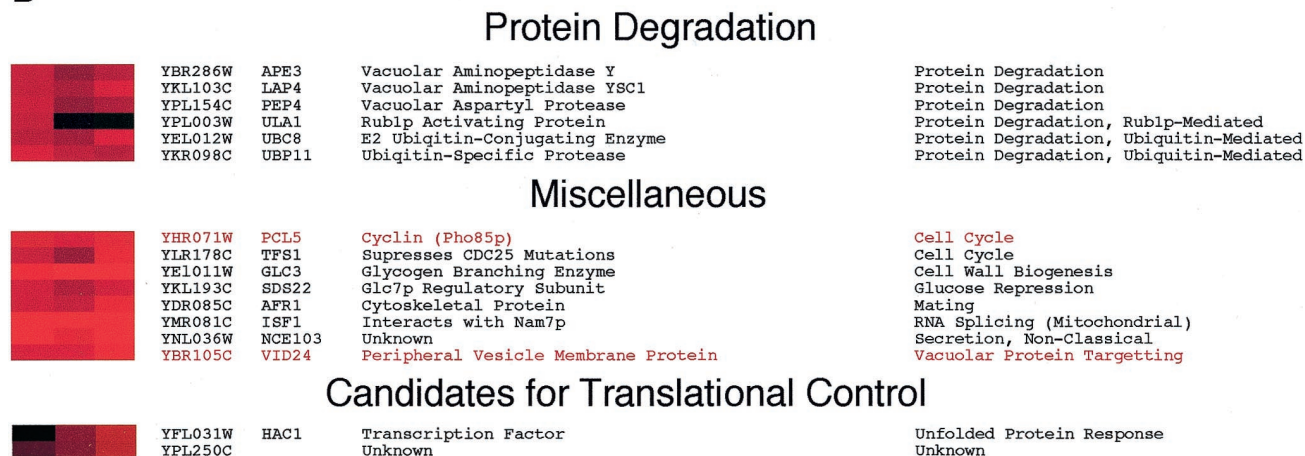|				
	YFL031W	HAC1	Transcription Factor	Unfolded Protein Response
	YPL250C		Unknown	Unknown

FIG. 5. Characterized genes whose relative mRNA abundances increase following a transfer to glycerol medium. Total and polysomal RNA levels were analyzed and displayed as described in the legend to Fig. 2. Genes selected for this figure were induced at least threefold at 10 min after a shift to glycerol medium. Exceptions were *MIG1*, *SNF3*, *APE3*, *LAP4*, *PEP4*, *ULA1*, and *UBC8*, all of which were induced at least 2.5-fold. The induction of *YAK1* and *YGP1* mRNAs was confirmed in a separate experiment. Grouping of genes was based on data available from the Yeast Protein Database (http://www.proteome.com). Gene names highlighted in red were induced specifically after an abrupt transfer from glucose to glycerol medium, but not during the diauxic shift 13. Glc7p, glycogen synthase phosphatase; TCA, tricarboxylic acid; GABA, γ-aminobutyric acid.

polysomal mRNA was compared to that of mRNA isolated from the nonpolysomal fractions, designated mRNP (Fig.), following a 0-, 5-, or 10-min incubation in glycerol medium. This analysis revealed a substantial redistribution of polysomal RP mRNAs into nonpolysomal fractions after the carbon source shift.

The data obtained from the cDNA microarray analysis were corroborated by monitoring the abundance and polysomal distribution of individual RP mRNAs by Northern analysis. Many RP ORFs are rather small and are occupied by only a few translating ribosomes. For this reason, we chose to examine the polysomal association of RP mRNAs containing ORFs with more than 500 nucleotides. Such RP ORFs are occupied by four to six ribosomes when cells are grown in glucose medium (see Fig. 3B). Figure 3A shows that, in contrast to that of *ADH1* mRNA, the total abundances of five individual RP mRNAs had decreased by 10 min after the carbon source shift. In addition, all five RP mRNAs relocalized from polysomal fractions 9 and 10 to monosomal fraction 6 and to nonpolysomal fraction 2 (Fig. 3B). Quantitation (Fig. 3C) showed that RP mRNAs occupied four to six ribosomes during growth in glucose medium and one ribosome after the shift to glycerol medium, suggesting a 70% reduction in the translation rate for these RP mRNAs. In contrast, *ADH1* mRNA was occupied by 9 to 11 ribosomes/mRNA in glucose medium, compared to 6 to 8 ribosomes/mRNA in glycerol medium (Fig. 3B and C), indicating a reduction in translation rate of approximately 30%. Similar observations were made when the polysomal distributions of approximately 70 individual mRNA species were examined (K. Kuhn, unpublished data). *ACT1* mRNA, which sediments somewhat diffusely with lower-molecular-weight polysomes after a carbon source shift (Fig. 1), contains an unusually long 5′ noncoding region which may negatively affect the translation initiation rate under global translational repression conditions. Overall, these findings indicate that the carbon

source shift resulted in a rapid loss of RP mRNAs from polysome fractions. Polysomal loss of RP mRNAs was more pronounced than that of other, non-RP mRNAs.

Lowering the abundance of an mRNA after carbon shift does not decrease its translational efficiency. It is known that transcription of RP genes is regulated under certain stress situation (34). Employing cDNA microarrays, it was found that the overall abundances of all yeast RP mRNAs diminished following a rapid shift from glucose to glycerol, suggesting that RP gene promoters were downregulated after the carbon shift. Thus, it could be argued that preexisting RP mRNAs, synthesized before the carbon source shift, were translated less efficiently after the carbon source shift. To examine this possibility, we monitored the translation of a reporter mRNA whose synthesis was controlled by a tetracycline-repressible transcription system (TetR) (3). Briefly, a *URA3* ORF-containing cDNA containing the 5′ and 3′ noncoding regions of the *CYC1* gene was inserted downstream of the TetR promoter. The resulting plasmid, p(5′cyc-ura3-cyc3′), was transformed into yeast strain CML240 (3). The relative abundance and polysomal association of the *URA3* reporter mRNA were monitored following a shift from glucose medium to glycerol medium to which doxycycline had been added to silence the transcription of the reporter gene. Figure 4A shows that preexisting reporter mRNA decayed with a turnover rate of approximately 30 min. However, *URA3* mRNA displayed similar polysomal distribution profiles in untreated cells and in doxycycline-treated cells containing smaller amounts of *URA3* mRNA (Fig. 4B), indicating that the efficiency of translation of *URA3* mRNA synthesized before the carbon shift was similar to that of mRNA synthesized after the carbon source switch. Thus, transcriptional inhibition after the carbon source shift does not in itself affect the efficiency with which an mRNA is translated.

Altered abundances and polysomal distributions of individual mRNAs reveal induction of specific intracellular pathways
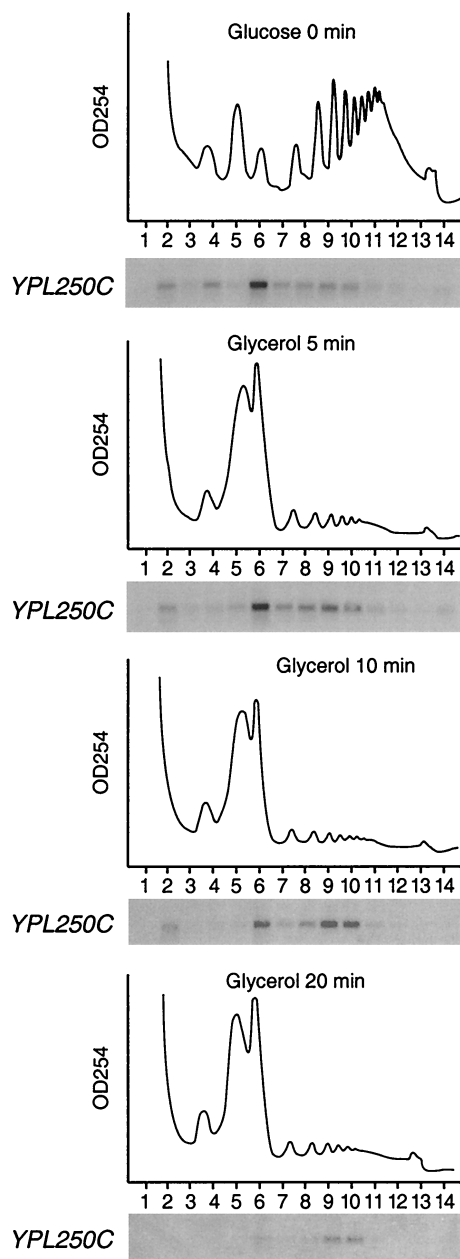
FIG. 6. *YPL250C* mRNA sediments with polysomes at a time when global translation rates are reduced: time course of *YPL250C* polysome association from cultures grown exclusively in glucose or shifted to glycerol for 20 min.

after the carbon source shift. The cDNA microarray analysis revealed many differences in mRNA abundance and polysomal representation in the approximately 6,275 genes examined. The relative abundances of 610 mRNAs increased by more than twofold after the shift to glycerol medium. Figure 5 lists examples of genes with known functions whose mRNA abundances had increased at least threefold by 10 min after the carbon source shift. The observed changes in gene expression were specific to the shift to glycerol medium, because expression of only 26 genes, all with unknown functions, increased

more than threefold when yeast cells were shifted into freshly prepared glucose medium (data not shown).

Although global translation was reduced, almost all of the mRNAs whose relative abundances increased were also associated with polysomes (Fig. 5). This observation was corroborated by analyzing the polysomal distributions of approximately 70 mRNA species (K. Kuhn, unpublished data). Two exceptions were the transcripts encoding flavin adenine dinucleotide-dependent glycerol-3-phosphate dehydrogenase GUT2 (36) and the Rub1p-activating protein ULA1 (31), which did not accumulate on polysomes despite exhibiting increased abundance after the carbon source shift. As a rule, virtually every mRNA species that increased in relative abundance after the shift to glycerol medium was also actively translated, although they all sedimented with fewer polysomes than did mRNAs isolated from glucose-grown cells (K. Kuhn, unpublished observation). This analysis highlights the efficiency with which *S. cerevisiae* responds to environmental cues. Within 5 min, new genes are expressed, processed, exported, and translated.

Interestingly, Fuge et al. (17) and Dickson and Brown (14) found that despite a global decrease in the activity of the protein synthesis machinery, the translational efficiencies of several mRNAs remained unchanged in exponentially growing and stationary-phase yeast cells. These observations prompted us to search for mRNAs whose translational efficiency either remained unchanged or actually increased following the shift to glycerol medium.

Selective mobilization of *YPL250C* mRNA into polysomes after the carbon source shift. Two mRNA species showed little change in total abundance but increased abundance on polysomes after the carbon source shift (Fig. 5B). One of these mRNAs is encoded by the *YPL250C* gene. In cells grown continuously in glucose medium, *YPL250C* mRNA sedimented predominantly in fractions corresponding to mRNAs with a single bound ribosome (Fig. 6, fraction 6) and less frequently in fractions corresponding to mRNAs with two to six ribosomes (fractions 7 to 10), a biphasic distribution pattern that is indicative of a translationally repressed mRNA. After the shift to glycerol medium, however, the majority of the *YPL250C* mRNA sedimented in fractions corresponding to four to six ribosomes/mRNA (fractions 9 and 10). Even at 20 min after the carbon source shift, when the overall abundance of *YPL250C* mRNA had declined, most *YPL250C* mRNAs were still detected in fractions corresponding to four to six ribosomes/mRNA (Fig. 6). Addition of 10 mM EDTA to the sucrose gradient abolished cosedimentation of the *YPL250C* mRNA with fractions 6 to 10 (data not shown), supporting the notion that the presence of *YPL250C* mRNA in this region of the gradient resulted from its association with ribosomes. Furthermore, *YPL250C* is not translationally enhanced following resuspension in glucose medium, ruling out the possibility that activation occurs in response to sedimentation or gravity stress (K. Kuhn, unpublished data). These observations indicate that *YPL250C* mRNA was selectively translated at an enhanced rate after the carbon source shift, at a time when overall translation of both preexisting and newly synthesized mRNAs was reduced (Fig. 1).

Activation of the bifunctional kinase-endonuclease Ire1p and the tRNA ligase Rlg1p after the carbon source shift. The
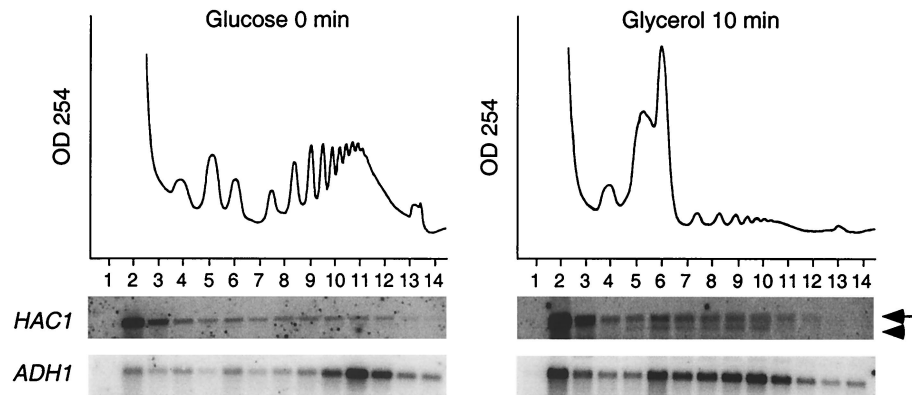
FIG. 7. A smaller species of *HAC1* RNA associates with polysomes 10 min after transfer from glucose to glycerol medium. Northern analysis with a *HAC1* ORF as a hybridization probe detected the full-length *HAC1*ᵘ mRNA (arrow) as well as a low-molecular-weight version of *HAC1*ⁱ (arrowhead) engaged with polysomes. The polysomal distribution of *ADH1*, taken from Fig. 1, is shown as a reference. Phosphorimages of the blots are shown below.

second example of an mRNA whose apparent polysomal association increased after a 10-min shift to glycerol, without significant changes in overall abundance, was *HAC1*, which encodes a transcription factor whose synthesis is stimulated as an essential part of the unfolded protein response (UPR) when unfolded proteins accumulate in the endoplasmic reticulum (ER) (7).

To verify the apparent increase in polysomal association of *Hac1* mRNA following the shift to glycerol, we reexamined the polysomal distribution of *Hac1* mRNA in cells that were continuously grown in glucose medium or shifted to glycerol medium. Cells grown continuously in glucose medium expressed a single 1.4-kb *HAC1* mRNA species, which sedimented predominantly with nonpolysomal fraction 2 and to some extent with polysomal fractions 8 to 11 (Fig. 7). Following the carbon source shift, the polysomal distribution of the 1.4-kb *HAC1* mRNA remained largely unchanged. However, a smaller, 1.2-kb species was detected predominantly in the polysomal fractions (Fig. 7). This 1.2-kb mRNA species is likely to have contributed to the increased relative abundance of polysome-associated *HAC1* mRNA observed in the cDNA microarray analysis. Since polysomal fractions from three glucose gradients and six glycerol gradients were processed to obtain equal (microgram) amounts of template RNA in the cDNA microarray analysis, the sample from the glycerol gradient contained a slight enrichment of mRNA (see Materials and Methods), which explains the relatively minor *HAC1* signal detected by Northern analysis (Fig. 7) compared with the more than two-fold-higher signal detected by the cDNA microarray analysis (Fig. 5B).

The appearance of the 1.2-kb *HAC1* mRNA was intriguing because *HAC1* expression is controlled by a regulated RNA splicing mechanism. The 1.4-kb unspliced *HAC1* mRNA, known as *HAC1*ᵘ (uninduced), can exit the nucleus and associate with ribosomes, but its translation has been reported to be attenuated at the elongation step (8). The results in Fig. 7 indicate that *HAC1*ᵘ mRNA sediments predominantly in nonpolysomal fraction 2, suggesting that translation of this mRNA species may also be blocked at the translation initiation step. Upon induction of the UPR pathway, *HAC1*ᵘ mRNA is spliced

to yield the 1.2-kb *HAC1*ᵘ (UPR-induced) mRNA, which is efficiently translated into Hac1pⁱ, whose C terminus differs from that of the Hac1pᵘ protein, encoded by *HAC1*ᵘ (8). Hac1pⁱ enters the nucleus and promotes transcription of genes that contain unfolded protein response elements in their promoters, such as *KAR2* and *PDI1*, whose products facilitate protein folding in the ER (reviewed in references 7 and 37).

To determine whether the 1.2-kb RNA species observed in the polysome profile (Fig. 7) was the spliced *HAC1*ⁱ mRNA, oligodeoxynucleotide primers were designed to distinguish between the unspliced and spliced versions of the *HAC1* mRNA. In cells grown continuously in glucose medium, *HAC1* mRNA was found to be predominantly unspliced (Fig. 8). Following transfer to glycerol medium, both unspliced and spliced (7, 37) *HAC1* mRNAs could be detected (Fig. 8). The spliced *HAC1* mRNA was transient, however, and it could not be detected by 45 min after the shift to glycerol medium. None of the known targets of Hac1pⁱ (e.g., *KAR2* or *PDI*) was detectably induced at this time after the carbon source shift (K. Kuhn, unpub-
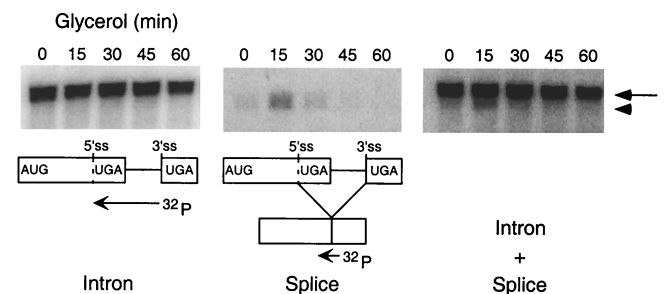

FIG. 8. *HAC1* mRNA is transiently spliced following glucose depletion. Total RNA was isolated from glycerol-shifted cultures at intervals during a 1-h time course and hybridized either with radiolabeled *Hac1* intron, with a small deoxyoligonucleotide that recognizes the *Hac1* splice junction ("Splice"), or with a mixture of intron and splice probes (Intron + Splice). The "splice" deoxyoligonucleotide is 18 nucleotides in length, with 9 nucleotides of complementarity to the spliced termini of each exon. ³²P-labeled probes are displayed. Phosphorimages of the blots are at top. Full-length *HAC1* mRNA (arrow) and the spliced *HAC1* (arrowhead) are indicated in the phosphorimage.
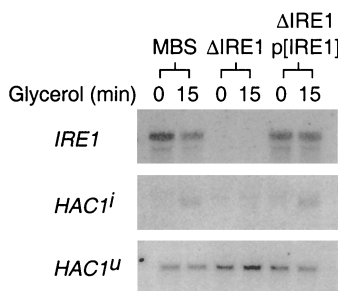
FIG. 9. The presence of *IRE1* is required for the transient splicing of *HAC1* mRNA. Total RNAs were isolated from strain MBS, a ΔIRE1 strain (yCS243a), and the ΔIRE1/p(IRE1) strain transformed with a functional copy of *IRE1* (pCS110). Northern blots were hybridized with either radiolabeled full-length *IRE1* cDNA or the "splice" oligodeoxynucleotide described in the legend to Fig. 8. Phosphorimages of the blots are shown.

lished data). Thus, although the appearance of polysome-associated *HAC1*i mRNA suggests that some Hac1pi may have been produced, its production was not accompanied by a transcriptional induction of the UPR response. Splicing of *HAC1*u mRNA is tightly regulated in the cell; it is induced by the accumulation of misfolded proteins in the ER and occurs by a nonconventional splicing mechanism mediated by two proteins, a bifunctional Ire1p kinase-endonuclease encoded by *IRE1* and a tRNA ligase encoded by *RLG1* (10, 25, 38). To determine whether Ire1p is required for the accumulation of *HAC1*i following the carbon source shift, splicing of *HAC1* mRNA in strains that contained or lacked *IRE1* was monitored. In contrast to the Ire1p-expressing strain MBS, the *IRE1* deletion strain ΔIRE1 failed to accumulate spliced *HAC1*i mRNA after the shift to glycerol medium (Fig. 9). Transformation of this strain with a plasmid expressing *IRE1* restored the accumulation of spliced *HAC1*i mRNA. All strains expressed detectable levels of unspliced *HAC1*u mRNA, indicating that the failure of the ΔIRE1 strain to produce spliced *HAC1*i mRNA was not due to low levels of unspliced *HAC1*u precursor mRNA. Thus, splicing of *HAC1*u mRNA after the carbon source shift appears to be mediated by the same Ire1p-dependent pathway that is involved in the UPR.

DISCUSSION

Following an abrupt shift from a fermentable to a nonfermentable carbon source, *S. cerevisiae* displays a diverse array of adaptive changes in gene expression at both the transcriptional and translational levels. The shift from a fermentable carbon source, glucose, to a nonfermentable carbon source, glycerol, resulted in a marked reduction in overall translation of mRNAs. The accumulation of 80S monosomes and ribosomal subunits after the carbon source shift indicated that the initiation phase of translation was inhibited. Two major mechanisms of down-regulating global translation initiation in *S. cerevisiae* have been described. In the first case, amino acid starvation induces phosphorylation of initiation factor eIF2α at serine 51 by the Gcn2p kinase, which results in a reduced concentration of 40S subunits, which carry initiator tRNA-eIF2 complexes, and subsequent derepression of *GCN4* mRNA translation (20). In the second case, induction of a diauxic shift by gradual glucose

exhaustion leads to degradation of initiation factor eIF4G (4), resulting in limiting concentrations of the cap-binding protein complexes needed to recruit 40S subunits onto mRNAs. In the case of the rapid shift from glucose to glycerol medium described here, translational inhibition was still observed in a yeast strain that expressed a mutated eIF2α whose phosphorylation site at serine 51 had been changed to alanine. In addition, eIF4G was not degraded after shifting *S. arevisiae* from glucose to glycerol medium at a time when translation was markedly depressed (K. Kuhn, unpublished data). Therefore, the mechanism of global translational repression that occurs following a rapid withdrawal of glucose must differ from that described during amino acid starvation or the diauxic shift. Recently, mutants in the cyclic-AMP-dependent kinase pathway have been shown to be resistant to translational inhibition after glucose withdrawal (1), suggesting that this signaling pathway is involved in translational regulation. We noted an increased abundance of several mRNAs encoding catalytic subunits of the cyclic-AMP-dependent kinase protein kinase A (PKA) upon carbon source shift (*TPK1* [4.1-fold], *TPK2* [3.8-fold], and *TPK3* [1.5-fold]). In addition, the relative abundance of the *BCY1* mRNA, which encodes the PKA regulatory subunit, was also induced twofold. These findings support the hypothesis by Ashe et al. (1) that increased concentration and activity of PKA can play a role in the inhibition of translation following a shift from a fermentable to a nonfermentable carbon source.

Loss of polysome-associated RP mRNAs after a shift to glycerol. Mammalian RP mRNAs contain terminal oligopyrimidine (5′ TOP) sequence elements in their 5′ noncoding regions that can negatively regulate translation initiation, particularly during serum starvation (reviewed in reference 33). In contrast, yeast RP mRNAs do not contain 5′ TOP elements, nor do they contain any obvious consensus sequences in their 5′ noncoding regions. With the exception of L30 mRNA, whose translation is negatively regulated by its encoded product Rpl30p (11), yeast RP mRNAs are generally not thought to be under translational control (33).

Curiously, all yeast RP mRNAs redistributed from polysomes to monosomes and untranslated mRNPs within 5 min after the shift to glycerol medium, suggesting that RP mRNAs are coordinately regulated at the translational level. Furthermore, we have shown that the reduced rate of ribosomal loading is not due to an inhibition of RP gene transcription. To gain information about the mechanism of the marked translational repression of RP mRNAs after a carbon shift, translation studies using a reporter mRNA containing the noncoding regions of *RPL15* were initiated. Preliminary experiments showed that the 3′ noncoding region of *RPL15*, but not its short 5′ noncoding region, mimicked the overall 80S and polysomal distribution pattern seen with endogenous *RPL15* mRNA during growth in glycerol (K. Kuhn, unpublished observation). Thus, signals for translational repression after a carbon shift may reside in the 3′ noncoding regions of RP mRNAs.

Translational regulation of *YPL250C* mRNA. *YPL250C* mRNAs were predominantly associated with an increased number of ribosomes following the transfer from glucose to glycerol medium. The mechanism by which *YPL250C* mRNAs selectively recruit ribosomes when the overall activity of the translational apparatus is diminished is being investigated. Prelim-

inary results have indicated that the 3′ noncoding region of the *YPL250C* mRNA is sufficient to mobilize a reporter mRNA into polysomes during glycerol-induced translational inhibition (K. Kuhn, unpublished data). Detailed characterization of the 3′ noncoding region in *YPL250C* mRNA will likely provide clues to the mechanism by which this mRNA confers preferential polysomal association to *YPL250C* mRNAs after the carbon source shift. A BY4742 strain with a *YPL250C* gene knockout mutation (Research Genetics) was viable and, when grown on glucose or glycerol medium, displayed a phenotype similar to that of the parent BY4742 and MBS strains used in this study. However, overexpression of YPL250C protein led to a slow-growth phenotype (K. Kuhn, unpublished data), implying that *YPL250C* gene expression may be tightly regulated under normal growth conditions. Nevertheless, the predicted 136 ORF-encoded *YPL250C* gene product is not absolutely essential for adaptation to a nonfermentable carbon source.

Splicing of *HAC1*ᵘ mRNA. Following the shift from glucose to glycerol medium, *HAC1*ᵘ transcripts were spliced by an Ire1p-dependent mechanism. *HAC1*ⁱ mRNA accumulation was transient, however, and none of the known genes in the UPR pathway was detectably induced (data not shown). Alternatively, the apparent activation of Ire1p following the carbon source shift, with no obvious consequence to the UPR pathway, raises the possibility that the regulatory function of Ire1p, and perhaps Hac1p, may not be solely devoted to the UPR and may influence expression of previously unrecognized target genes. The transient nature of *HAC1* mRNA splicing and translation may reflect an adaptive response to environmental stress. Transient translational events may occur in a stressed organism as an intermediate response toward adaptation to a new equilibrium state. Nevertheless, if one considers that the average cell cycle of *S. cerevisiae*, when grown in minimal medium, lasts approximately 120 min, then a significant amount of protein may have been synthesized within 15 min.

Translation of *HAC1*ᵘ has been shown to be regulated during the elongation step (reviewed in references 7 and 37). It is interesting, however, that the polysomal distribution of *HAC1*ᵘ mRNA in Fig. 7 differs from that detailed in previously published reports, in which the majority of *HAC1*ᵘ mRNA sedimented with polysomes while only a minor fraction (~20%) sedimented with low-density mRNP fractions (8, 10). In contrast, we have routinely observed an accumulation of *HAC1*ᵘ mRNA in the mRNP fractions (Fig. 7, fractions 2 and 3) and very little sedimentation of this unspliced mRNA with polysome fractions. We are uncertain about the origin of this discrepancy. *HAC1*ᵘ mRNA is known to be distributed throughout the cytoplasm in punctate clusters (8). Although the composition of these clusters is presently unknown, the *HAC1*ᵘ mRNA within these clusters may be difficult to extract. Our findings argue that translation of *HAC1*ᵘ mRNA is blocked at the initiation step, in addition to the previously reported elongation step, and that there may be a cytoplasmic pool of *HAC1*ᵘ mRNA which is sequestered as a translationally inactive mRNP complex.

An interesting observation has connected the protein secretory pathway with ribosome biosynthesis. The continued functioning of the secretory pathway has been shown to be essential for ribosome biosynthesis, because inhibition of the secretory pathway reduces transcription of genes encoding RP mRNAs

(34). The fact that components of the ER are affected by the carbon source shift is exemplified by the activation of the bifunctional kinase-endonuclease Ire1p and the tRNA ligase Rlg1p.

The genomic response of *S. cerevisiae* to nutritional change was very rapid. By combining polysomal fractionation with cDNA microarray analysis, we have primarily focused on the translational activity of thousands of individual mRNAs after a rapid depletion of glucose. Identification of individual mRNAs that are translationally controlled has historically relied on cumbersome analyses of suspected mRNA species. The cDNA microarray analysis has uncovered an mRNA species (*YPL250C*) that can be selectively translated during a global translational inhibition, as well as a coordinate regulation of an entire class of mRNAs (RP mRNAs). Activation of the bifunctional kinase-endonuclease Ire1p and the tRNA ligase Rlg1p after a carbon source shift was confirmed by the appearance of spliced *HAC1* mRNAs in polysomal fractions. This latter finding exemplifies the effectiveness of the cDNA microarray, which can allow the detection of multiple levels of regulation that operate in the genomic response of an organism to nutritional change.

REFERENCES

1. **Ashe, M. P., S. K. De Long, and A. B. Sachs.** 2000. Glucose depletion rapidly inhibits translation initiation in yeast. Mol. Biol. Cell **11:**833–848.
2. **Ausubel, F. M., R. Brent, R. E. Kingston, D. D. Moore, J. G. Seidman, J. A. Smith, and K. Struhl (ed.).** 1994. Current protocols in molecular biology. Greene Publishing Associates and John Wiley & Sons, New York, N.Y.
3. **Belli, G., E. Gari, L. Piedrafita, M. Aldea, and E. Herrero.** 1998. An activator/repressor dual system allows tight tetracycline-regulated gene expression in budding yeast. Nucleic Acids Res. **26:**942–947. (Erratum, **26:**1855.)
4. **Berset, C., H. Trachsel, and M. Altmann.** 1998. The TOR (target of rapamycin) signal transduction pathway regulates the stability of translation initiation factor eIF4G in the yeast *Saccharomyces cerevisiae*. Proc. Natl. Acad. Sci. USA **95:**4264–4269.
5. **Boucherie, H.** 1985. Protein synthesis during transition and stationary phases under glucose limitation in *Saccharomyces cerevisiae*. J. Bacteriol. **161:**385–392.
6. **Carter, M. S., K. M. Kuhn, and P. Sarnow.** 2000. Cellular internal ribosome entry site elements and the use of cDNA microarrays in their investigation, p. 615–635. *In* N. Sonenberg, J. W. B. Hershey, and M. B. Mathews (ed.), Translational control of gene expression. Cold Spring Harbor Laboratory Press, Cold Spring Harbor, N.Y.
7. **Chapman, R., C. Sidrauski, and P. Walter.** 1998. Intracellular signaling from the endoplasmic reticulum to the nucleus. Annu. Rev. Cell Dev. Biol. **14:**459–485.
8. **Chapman, R. E., and P. Walter.** 1997. Translational attenuation mediated by an mRNA intron. Curr. Biol. **7:**850–859.
9. **Chu, S., J. DeRisi, M. Eisen, J. Mulholland, D. Botstein, P. O. Brown, and I. Herskowitz.** 1998. The transcriptional program of sporulation in budding yeast. Science **282:**699–705.
10. **Cox, J. S., and P. Walter.** 1996. A novel mechanism for regulating activity of a transcription factor that controls the unfolded protein response. Cell **87:**391–404.
11. **Dabeva, M. D., and J. R. Warner.** 1993. Ribosomal protein L32 of *Saccharomyces cerevisiae* regulates both splicing and translation of its own transcript. J. Biol. Chem. **268:**19669–19674.
12. **DeRisi, J. L., and V. R. Iyer.** 1999. Genomics and array technology. Curr. Opin. Oncol. **11:**76–79.
13. **DeRisi, J. L., V. R. Iyer, and P. O. Brown.** 1997. Exploring the metabolic and

genetic control of gene expression on a genomic scale. Science **278:**680–686.

14. **Dickson, L. M., and A. J. Brown.** 1998. mRNA translation in yeast during entry into stationary phase. Mol. Gen. Genet. **259:**282–293.

15. **Eisen, M. B., and P. O. Brown.** 1999. DNA arrays for analysis of gene expression. Methods Enzymol. **303:**179–205.

16. **Eisen, M. B., P. T. Spellman, P. O. Brown, and D. Botstein.** 1998. Cluster analysis and display of genome-wide expression patterns Proc. Natl. Acad. Sci. USA **95:**14863–14868.

17. **Fuge, E. K., E. L. Braun, and M. Werner-Washburne.** 1994. Protein synthesis in long-term stationary-phase cultures of *Saccharomyces cerevisiae*. J. Bacteriol. **176:**5802–5813.

18. **Gorenstein, C., and J. R. Warner.** 1976. Coordinate regulation of the synthesis of eukaryotic ribosomal proteins. Proc. Natl. Acad. Sci. USA **73:**1547–1551.

19. **Herruer, M. H., W. H. Mager, H. A. Raue, P. Vreken, E. Wilms, and R. J. Planta.** 1988. Mild temperature shock affects transcription of yeast ribosomal protein genes as well as the stability of their mRNAs. Nucleic Acids Res. **16:**7917–7929.

20. **Hinnebusch, A. G.** 1997. Translational regulation of yeast GCN4. A window on factors that control initiator-tRNA binding to the ribosome. J. Biol. Chem. **272:**21661–21664.

21. **Iizuka, N., L. Najita, A. Franzusoff, and P. Sarnow.** 1994. Cap-dependent and cap-independent translation by internal initiation of mRNAs in cell extracts prepared from *Saccharomyces cerevisiae*. Mol. Cell. Biol. **14:**7322–7330.

22. **Johannes, G., and P. Sarnow.** 1998. Cap-independent polysomal association of natural mRNAs encoding c-myc, BiP, and eIF4G conferred by internal ribosome entry sites. RNA **4:**1500–1513.

23. **Johnston, M.** 1999. Feasting, fasting and fermenting. Glucose sensing in yeast and other cells. Trends Genet. **15:**29–33.

24. **Johnston, M., and M. Carlson** 1992. Regulation of carbon and phosphate utilization, p. 193–281. *In* E. W. Jones, J. R. Pringle, and J. R. Broach (ed.),. The molecular and cellular biology of the yeast *Saccharomyces*, vol. 2. Gene expression. Cold Spring Harbor Laboratory Press, Cold Spring Harbor, N.Y.

25. **Kawahara, T., H. Yanagi, T. Yura, and K. Mori.** 1997. Endoplasmic reticulum stress-induced mRNA splicing permits synthesis of transcription factor Hac1p/Ern4p that activates the unfolded protein response. Mol Biol. Cell **8:**1845–1862.

26. **Kief, D. R., and J. R. Warner.** 1981. Coordinate control of syntheses of ribosomal ribonucleic acid and ribosomal proteins during nutritional shift-up in *Saccharomyces cerevisiae*. Mol. Cell. Biol. **1:**1007–1015.

27. **Kim, C. H., and J. R. Warner.** 1983. Mild temperature shock alters the transcription of a discrete class of *Saccharomyces cerevisiae* genes. Mol. Cell. Biol. **3:**457–465.

28. **Lagunas, R.** 1979. Energetic irrelevance of aerobiosis for *S. cerevisiae* growing on sugars. Mol. Cell. Biochem. **27:**139–146.

29. **Li, B., C. R. Nierras, and J. R. Warner.** 1999. Transcriptional elements involved in the repression of ribosomal protein synthesis. Mol. Cell. Biol. **19:**5393–5404.

30. **Li, B., and J. R. Warner.** 1996. Mutation of the Rab6 homologue of *Saccharomyces cerevisiae*, YPT6, inhibits both early Golgi function and ribosome biosynthesis J. Biol. Chem. **271:**16813–16819.

31. **Liakopoulos, D., G. Doenges, K. Matuschewski, and S. Jentsch.** 1998. A novel protein modification pathway related to the ubiquitin system. EMBO J. **17:**2208–2214.

32. **Mascorro-Gallardo, J. O., A. A. Covarrubias, and R. Gaxiola.** 1996. Construction of a CUP1 promoter-based vector to modulate gene expression in *Saccharomyces cerevisiae*. Gene **172:**169–170.

33. **Meyuhas, O., D. Avni, and S. Shama** 1996. Translational control of ribosomal protein mRNAs in eukaryotes, p. 363–388. *In* J. W. B. Hershey, M. B. Mathews, and N. Sonenberg (ed.), Translational control. Cold Spring Harbor Laboratory Press, Cold Spring Harbor, N.Y.

34. **Mizuta, K., and J. R. Warner.** 1994. Continued functioning of the secretory pathway is essential for ribosome synthesis. Mol. Cell. Biol. **14:**2493–2502.

35. **Planta, R. J.** 1997. Regulation of ribosome synthesis in yeast. Yeast **13:**1505–1518.

36. **Ronnow, B., and M. C. Kielland-Brandt.** 1993. GUT2, a gene for mitochondrial glycerol 3-phosphate dehydrogenase of *Saccharomyces cerevisiae*. Yeast **9:**1121–1130.

37. **Sidrauski, C., R. Chapman, and P. Walter.** 1998. The unfolded protein response: an intracellular signalling pathway with many surprising features. Trends Cell Biol. **8:**245–249.

38. **Sidrauski, C., J. S. Cox, and P. Walter.** 1996. tRNA ligase is required for regulated mRNA splicing in the unfolded protein response. Cell **87:**405–413.

39. **Werner-Washburne, M., J. Becker, J. Kosic-Smithers, and E. A. Craig.** 1989. Yeast Hsp70 RNA levels vary in response to the physiological status of the cell. J. Bacteriol. **171:**2680–2688.

40. **Werner-Washburne, M., E. Braun, G. C. Johnston, and R. A. Singer.** 1993. Stationary phase in the yeast *Saccharomyces cerevisiae*. Microbiol. Rev. **57:**383–401.

41. **Werner-Washburne, M., E. L. Braun, M. E. Crawford, and V. M. Peck.** 1996. Stationary phase in *Saccharomyces cerevisiae*. Mol. Microbiol. **19:**1159–1166.